Physics – Uspekhi **61** (5) 435 – 448 (2018)

60th ANNIVERSARY OF THE BUDKER INSTITUTE OF NUCLEAR PHYSICS (BINP), SB RAS

PACS number: 41.60.Cr

Free electron lasers and their development at the Budker Institute of Nuclear Physics, SB RAS

N A Vinokurov, O A Shevchenko

DOI: https://doi.org/10.3367/UFNe.2018.02.038311

Contents

Abstract. This review is devoted to free electron lasers (FELs) and their development research at the Budker Institute of Nuclear Physics (INP), SB RAS. Basic principles of FEL physics are considered. Selected studies from forty years of research are presented. The unique Novosibirsk FEL research facility is briefly described.

Keywords: free electron laser, undulator, coherent radiation, electron beam

1. Introduction

This review describes free electron lasers (FELs). This field of applications of electron beams is important and interesting by itself. For us, however, it is also an incentive to consider a number of interesting physical phenomena demonstrating the operation of the general laws of electrodynamics and the special relativity.

Free-electron lasers convert the energy of ultrarelativistic electrons (i.e., electrons with an energy exceeding many times their rest energy) into electromagnetic radiation energy. These lasers can emit monochromatic radiation at any wavelength in the range from 0.1 nm to 1 mm (seven orders of magnitude!), and this wavelength can relatively rapidly be tuned by several tens of a percent.

To provide a strong (resonance) interaction of relativistic electrons with an electromagnetic wave, their trajectory, which is a straight line in a vacuum, is made slightly periodically curved in the form of a spiral or a wavy line. A device with a magnetic field required to create such a trajectory is called an undulator or a wiggler (see, for example, review [1]). If an electron lags behind an electromagnetic wave by one wavelength after propagating over one period of the trajectory (the so-called synchronism condition), such a wave can efficiently decelerate the electron along the entire wavy trajectory. In this case, the electron radiation field will be added to the field of the initial wave, enhancing the latter (because the electron is decelerated, it loses own energy, which is transferred to the wave).

The operation principle of FELs consists in the following. Consider an electron beam and an electromagnetic wave entering an undulator (Fig. 1). If the electron energy and wavelength satisfy the synchronism condition, half the electrons begin to lose their energy, while the other half entering the undulator later by the wave half-period acquire

N A Vinokurov Budker Institute of Nuclear Physics,
Siberian Branch of the Russian Academy of Sciences,
prosp. Akademika Lavrent'eva 11, 630090 Novosibirsk;
Russian Federation
Novosibirsk State University,
ul. Pirogova 1, 630090 Novosibirsk, Russian Federation
E-mail: vinokurov@inp.nsk.ru
O A Shevchenko Institute of Nuclear Physics,
Siberian Branch of the Russian Academy of Sciences,
prosp. Akademika Lavrent'eva 11, 630090 Novosibirsk,
Russian Federation

Received 15 January 2018
Uspekhi Fizicheskikh Nauk **188** (5) 493 – 507 (2018)
DOI: https://doi.org/10.3367/UFNr.2018.02.038311
Translated by M N Sapozhnikov; edited by A Radzig

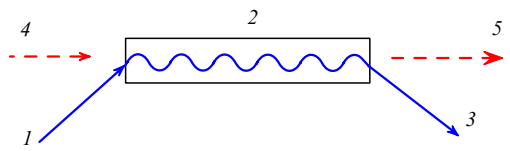

Figure 1. Schematic of an FEL amplifier: (*1*) input electron beam, (*2*) undulator, (*3*) waste electrons, (*4*) input electromagnetic wave, and (*5*) amplified wave.

energy. Thus, at first, the electron energy in average does not change but is modulated, i.e., the beam is decomposed into half-wavelength-thick slices with alternating energy deviations from the initial energy. Particles with a smaller energy move more slowly, while particles with a greater energy move faster. Because of this, 'fast' slices will catch up with 'slow' slices, thereby producing the electron density modulation with a spatial period equal to the wavelength. Then, the situation observed in the first half of the undulator is repeated: some of the half-wavelength beam slices are decelerated by the electromagnetic wave, whereas the other slices are accelerated, but now slices with the higher density of particles lose energy, while slices with the lower density acquire energy. As a result, the average electron energy decreases, whereas the electromagnetic wave power increases.

In this way, FELs amplify electromagnetic radiation. If, as in many other lasers, two mirrors are mounted on the system's axis to the left and right of the undulator, the wave will circulate between them and, passing many times through the undulator with electrons, will be amplified each time. Of course, an increase in the radiation intensity is limited. One of the reasons for the intensity limitation (saturation) might be the almost complete bunching of electrons in the second half of the undulator. In this case, a further increase in the radiation power at the FEL input leads to a decrease of bunching (debunching), thereby reducing power transferred from the beam to radiation.

To explain the content of the three previous paragraphs, we should recall the fundamentals of electrodynamics and discuss processes proceeding in FELs in more detail.

2. Spontaneous, stimulated, and coherent radiation

Electromagnetic waves are emitted by electrons moving with acceleration. The radiation power of one electron is very low on the macroscopic scale. This means that for practical applications it is necessary to involve many electrons. For example, in a candle flame and a gas-discharge lamp a huge number of atoms of incandescent gas (and an electron in each atom moving around a nucleus) emit electromagnetic radiation. To simplify the picture, each atom can be mentally replaced by a charge fixed at the end of a spring. At some instant of time t_n, a charge with the number n is displaced from the equilibrium position and then begins to oscillate. The charge moving with acceleration emits radiation and loses its energy. As a result, the charge oscillations and radiation terminate after some time.

Another example of an elementary emitter is an electron entering a finite-length undulator at the instant t_n. For simplicity, we assume that all the 'splashes' of the electric field $E_1(t-t_n)$ are the same and differ only in their 'switching on' time t_n. The radiation field of many charges will be equal to the sum of splashes from each emitter:[1] $E(t) = \sum_n E_1(t-t_n)$. Let us transmit this signal through a monochromator or a frequency filter (Fig. 2). It is well known (see, for example, textbook [2]) that a monochromator stretches each radiation splash. We will assume that it transforms the flash $E_1(t-t_n)$ to the wave packet $a\cos[\omega(t-t_n)]\,\vartheta(t-t_n)\times\vartheta(T-t+t_n)$, extending from 0 to T ($\vartheta(t)=1$ for $t\geqslant 0$, and

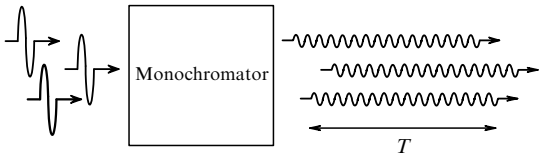

Figure 2. Radiation 'splashes' from three emitters pass through a monochromator. Wave packets with a long duration T and the carrier frequency to which the monochromator is tuned escape from the monochromator.

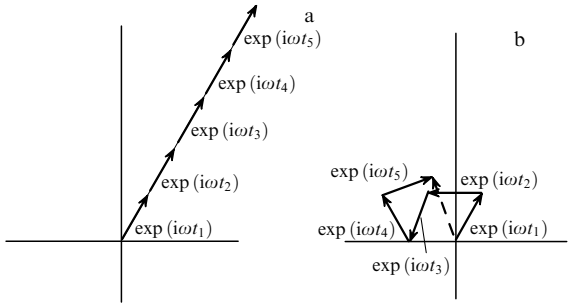

Figure 3. Summation of spectral harmonics from five emitters: (a) coherent radiation, and (b) 'typical' case. The sum is shown by the dashed arrow.

$\vartheta(t)=0$ for $t<0$). Then, the output signal of the monochromator has the form

$$E_{\mathrm{M}}(t) = a\sum_n \cos\left[\omega(t-t_n)\right]\vartheta(t-t_n)\,\vartheta(T-t+t_n)$$
$$= \mathrm{Re}\left[\exp(-\mathrm{i}\omega t)\,a\sum_n \exp(\mathrm{i}\omega t_n)\,\vartheta(t-t_n)\,\vartheta(T-t+t_n)\right]. \quad (1)$$

It follows from formula (1) that the complex amplitude of the signal $\sum_n a\exp(\mathrm{i}\omega t_n)$ is the sum of complex amplitudes of individual emitters, taking into account only emitters with $t-T<t_n<t$. If we are dealing with a stationary process, the mean operation frequency ν of the emitters is known. Then, the mean number of summable amplitudes is $N=\nu T$. As a rule, this is a huge number. Moreover, by improving the spectral resolution of a monochromator, we increase its response duration T. Therefore, N infinitely increases in the limit of the ideal monochromator. To increase the signal spectral density proportional to the modulus squared of the field complex amplitude

$$\left|\sum_n a\exp(\mathrm{i}\omega t_n)\right|^2 = \sum_m\sum_n a^2\exp\left[\mathrm{i}\omega(t_n-t_m)\right], \quad (2)$$

it is necessary to choose all the emission moments of emitters so that the phases of harmonics ωt_n are the same (accurate to 2π), as shown in Fig. 3a. It is possible, for example, to inject electrons into an undulator with a time delay with respect to each other equal to the integer number q of periods, i.e., $2\pi q/\omega$. This is difficult to do, but is realized, in principle, in FELs (see below). When all elementary emitters are optimally synchronized (phased), coherent emission is said to take place.[2] In this case, the signal amplitude at the monochromator output is Na on average.

In the 'typical' case, contributions from individual emitters have different phases (Fig. 3b). Let us find the mean

[1] We assume here for simplicity that all the emitters are located at the same distance from a detector, and therefore the emitter coordinate is absent in the field argument.

[2] Unfortunately, the term 'coherence' is applied to many physical phenomena in different senses.

square of the modulus of signal complex amplitude (2), but first refine the term 'mean value'.

Remark about averaging. Consider a system characterized by N numbers, for example, $t_1, t_2, \ldots, t_N$. In the space of system's parameters, a nonnegative function $f(t_1, t_2, \ldots, t_N)$ normalized to unity is specified: $\int f \, \mathrm{d}t_1 \ldots \mathrm{d}t_N = 1$, where the integral is taken over the entire region of admissible values of system's parameters. This function is called the probability density or the distribution function. Its meaning is usually explained as follows. Assume that system's parameters are *a priori* unknown. We find them with the aid of some measurements. In addition, we assume that there are a very great number of equivalent copies of the system under study, and we measured the parameters of each of them. Then, the portion of copies entering a small N-dimensional parallelepiped described by inequalities $s_1 - \Delta t_1/2 < t_1 < s_1 + \Delta t_1/2, \ldots, s_N - \Delta t_N/2 < t_N < s_N + \Delta t_N/2$ (more exactly, its limit with an unlimited increase in the number of copies and an unlimited decrease in the parallelepiped size) is given by $f(s_1, \ldots, s_N)\Delta t_1 \ldots \Delta t_N$.

The probability density resembles Plato's reasoning about ideal subjects, which are more real than their imperfect embodiments that we observe. The 'embodiment' of the distribution function is histograms. The space of parameters is divided into finite regions, measurements are performed for a finite number of the system copies, and the number of copies entering the given region of the parameter space is counted.

The mathematical probability density is well defined, because it specifies the measure of sets in the parameter space. The mean value or mathematical expectation of a function $G(t_1, t_2, \ldots, t_N)$ is the number

$$\langle G \rangle = \int G f \, \mathrm{d}t_1 \ldots \mathrm{d}t_N \,. \tag{3}$$

We have now found out what is the mean. However, to calculate the average spectral density (2), the probability density should be known. First, let us assume that emitters are statistically independent. This means (by definition) that the probability density is a product of N functions, each of them depending only on one time t_n. In addition, because emitters are identical, these functions should also be identical. How does this occur? Consider, for example, electrons in an undulator which appeared from a cathode surface heated to a high temperature. As a rule, electrons adjacent in time escape from the parts of the surface separated by a rather large distance (a few millimeters). Therefore, the escape of one electron does not affect the motion of another electron. This is the case of the independent motion of different electrons. This independence can later be violated. For example, electrons emitted from the cathode are mutually pushed apart (the electric field of each electron changes the momenta of other electrons) and are 'aligned' approximately at the same distances from each other.[3] Then, the multiparticle distribution function will no longer decompose into single-particle factors.

Returning to the discussion of spontaneous, stimulated, and coherent emission, we make a further simplification by considering a stationary process in which all the probability densities are constant (i.e., are time-independent). Therefore,

[3] This phenomenon was used to suppress current fluctuations in the electron beams of low-noise traveling-wave tubes.

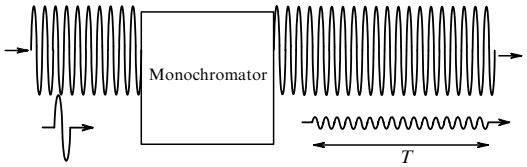

Figure 4. 'Splash' from an emitter and a monochromatic signal passing through a monochromator.

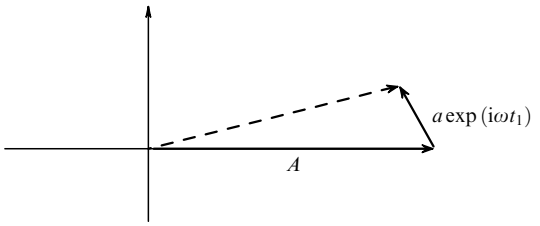

Figure 5. Summation of a spectral harmonic of an emitter with a monochromatic signal. The sum is shown by the dashed arrow.

$\langle \exp(\mathrm{i}\omega t_n) \rangle = 0$ and

$$\left\langle \left| \sum_n a \exp(\mathrm{i}\omega t_n) \right|^2 \right\rangle = \sum_n a^2 = Na^2 \,.$$

The latter equation implies that the average spectral radiation intensity of independent emitters is a sum of the spectral intensities of individual emitters. Notice that, in this case, we lose a lot in the spectral intensity (by the factor N) compared with that for coherent emission (when all the emitters are ideally synchronized).[4] The emission of an ensemble of statistically independent (unsynchronized) emitters is called spontaneous emission.

We will now somewhat change the experiment (Fig. 4). Along with the emitter, we also consider an 'external' plane monochromatic wave with the frequency to which the monochromator is tuned and the complex amplitude A. The output signal of the monochromator can also be shown in the vector diagram (Fig. 5).

The output signal power is proportional to

$$\left| A + a \exp(\mathrm{i}\omega t_1) \right|^2 = |A|^2 + 2 \,\mathrm{Re}\left[Aa \exp(-\mathrm{i}\omega t_1) \right] + a^2 \,,$$

i.e., is equal to the sum of the powers of the monochromatic signal, interference term, and spontaneous emission contribution a^2. By narrowing the frequency band of the monochromator, we reduce the emitter field amplitude a at the monochromator output. Because the transmitted signal energy $a^2 T$ is proportional to the transmission band $1/T$ of the monochromator, the amplitude a decreases as $1/T$ upon narrowing the monochromator transmission band. Therefore, the complex amplitude of the emitter signal for a good enough monochromator is much smaller than the monochro-

[4] In the case of the infinite duration of the process, the spectral density (the power limit at the monochromator output upon narrowing the monochromator band, i.e., for $N \to \infty$) of the undulator radiation from particles separated exactly by the time interval $2\pi/\omega_0$ has the form of an infinitely narrow peak, i.e., it is proportional to the delta function $\delta(\omega - \omega_0)$. It is said in this case that the radiation spectrum is discrete.

matic signal amplitude. In this case, the contribution of spontaneous emission to the energy transferred through the monochromator,

$$\left|A + a\exp\left(\mathrm{i}\omega t_1\right)\right|^2 T = |A|^2 T + 2\,\mathrm{Re}\left[Aa\exp\left(-\mathrm{i}\omega t_1\right)\right]T + a^2 T,$$

tends to zero, while the contribution from the interference term remains finite. If there are many emitters that are not synchronized with a monochromatic signal, then $\langle\exp\left(\mathrm{i}\omega t_1\right)\rangle = 0$. In this case, the averaging represents a summation over a large number of emitters followed by division of the result by the number of emitters. Thus, the interference term is zero on average, and the output power is the sum of the monochromatic signal power and spontaneous emission power rapidly decreasing upon narrowing the monochromator transmission band.

In fact, this is not always the case: a monochromatic wave, before entering a monochromator, could be in the same spatial region as an emitter and act on it. In this case, the motion of electrons in the emitter has changed, and this change depended on the external wave phase, so that the phases of the emitters somewhat shifted and the average interference term became, generally speaking, nonzero. If the total power decreased in this case, it is said that emitters absorb the external wave. Otherwise, they amplify it. This is the case of emerging the stimulated emission, which means that emitters release their energy to the radiation field faster than in the case of spontaneous emission in the absence of an external wave.

To move forward further, it is necessary to describe the particular mechanisms of synchronization of emitters by an external wave. Consider first the above-mentioned model of an atom — a charge on a spring. For such a model to be valid, the oscillator frequency should depend on the oscillation amplitude. This oscillator property, called nonisochronism, is quite common. For example, the oscillation frequency of a pendulum decreases with increasing oscillation amplitude. Another practically important example is electron rotation[5] in a uniform magnetic field with the frequency decreasing with increasing electron energy.

Thus, consider an ensemble of identical emitters oscillating first with the same amplitudes, with the oscillation frequency coinciding with the external wave frequency. Assume that emitters are first distributed over oscillation phases ωt_n uniformly, i.e., $\langle\exp\left(\mathrm{i}\omega t_n\right)\rangle = 0$. The initial distribution of oscillators in the phase–energy plane is plotted in Fig. 6a.

Because the energy transferred from an oscillator to the external wave is proportional to $2\,\mathrm{Re}\left[Aa\exp\left(-\mathrm{i}\omega t_n\right)\right]T$, half the oscillators lose their energy, while the other half acquires energy (Fig. 6b), and on average the energy exchange between oscillators and the wave is absent. However, the energy of each oscillator depends on its initial phase. The energy deviation changes in the oscillation frequency of the oscillator. Assume for definiteness that the frequency decreases with increasing energy. Then, the frequency of oscillators with phases close to zero increases, while the frequency of oscillators with phases close to π decreases. The phases of emitters losing energy will increase, whereas the phases of emitters acquiring energy will decrease. As a result, the phase distribution will become nonuniform after some time — we will get crowding near the phase $\pi/2$, and sparseness near the phase $-\pi/2$ (Fig. 6a). Because no energy exchange between the emitter and the wave takes place at these phases, neither amplification nor absorption occur. On the other hand, the phasing of emitters can be of interest in itself. For example, their emission will be coherent to some extent in the sense that the sum of their spectral harmonics will look like something intermediate between those presented in Figs 3a and b.

[5] Rotation is equivalent to oscillations over two coordinates.

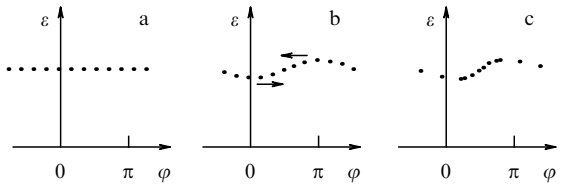

Figure 6. Phase grouping of oscillators in the wave field. (a) The initial state. All the oscillators have the same energies and are uniformly distributed in phase. (b) Some oscillators lost their energy, while others acquired it. The phase distribution is still almost uniform, but due to the energy dependence of the frequency, phases began to shift, as shown by arrows. (c) The phase shift gives rise to crowding near $\varphi = \pi/2$, and a rarefaction near $\varphi = -\pi/2$.

To transfer part of the oscillator energy to an external wave, i.e., to amplify the latter, it is necessary to shift the relative phase of oscillators (already with the nonuniform phase distribution) and the wave. This can be most simply performed by introducing the initial detuning (difference) of the wave frequency ω and oscillator frequencies $\Omega(\varepsilon_0)$. Then, the oscillator distributions shown in Fig. 6 will 'flow' in phase with the velocity $\Omega(\varepsilon_0) - \omega$. If the initial energy ε_0 slightly exceeds the synchronous energy ε_s at which the wave and oscillator frequencies coincide, then the above-mentioned velocity is negative and distributions 'flow' to the left. This means that crowding at the $\pi/2$ phase will shift for the time $\pi/[2(\omega - \Omega(\varepsilon_0))]$ to the zero phase where the energy extraction is maximal, while the rarefaction at $-\pi/2$ will shift to the π phase with a maximum rate of the energy gain. As in the zero-detuning case, some oscillators transfer their energy to the wave, while others extract energy from the wave, but now the amount of the former is larger. As a result, when the initial energy of oscillators exceeds the synchronous energy, the wave is amplified. On the contrary, for initial energies lower than the synchronous energy, the energy is absorbed (on the average) by emitting oscillators, and the external wave is attenuated. It should be noted that in both cases the average energy of emitters approaches the synchronous energy.

The simple model described above was proposed in the mid-20th century (see, for example, book [3] and references cited therein) and used by A V Gaponov-Grekhov and coworkers in the invention and development of a new class of electromagnetic radiation amplifiers — cyclotron resonance masers or gyrotrons. In these devices, electrons move in a uniform magnetic field along spiral trajectories. The rotating electrons emit at the cyclotron frequency. Gyrotrons take advantage of the stimulated emission of these electrons. Modern gyrotrons emit radiation with an average power of about 1 MW in the millimeter wavelength range.

Emitters in real systems have different initial energies. Then, to amplify an external signal, the number of emitters with an energy exceeding the synchronous energy must be greater than emitters with the lower energy. Such an initial state is called the 'inversion population'. This name is related to the fact that the distribution function in the thermody-

namic equilibrium decreases with energy (the so-called Gibbs distribution). Therefore, in nature, where the local thermodynamic equilibrium commonly takes place, the wave absorption processes dominate. The absorption of a wave by resonance particles was first described theoretically by L D Landau [4], who studied the damping of a longitudinal plasma wave. We can say that the Landau damping is caused by the absorption (i.e., by a stimulated process) of longitudinal plasma waves by plasma electrons.[6] For some nonequilibrium energy distributions of electrons in plasma, plasma waves can be amplified, i.e., such plasma states are unstable.

3. Stimulated undulator radiation

Consider stimulated undulator radiation in more detail. To clarify the mechanism of synchronization of electrons in the undulator, it is necessary to find out how an external electromagnetic wave affects the electron motion. Let us take a look at the simplest case of a planar undulator [1] with period $\lambda_w = 2\pi/k_w$, whose magnetic field has only one component $B_y = -B\cos(k_w z)$ in the xz plane, and an electron moving in this field along the trajectory:

$$x \approx \frac{K}{\gamma k_w}\cos(k_w z), \quad y = 0, \tag{4}$$

where γ is the relativistic factor (the ratio of the electron energy to its rest energy), $K = eB/(k_w mc^2)$ is the so-called undulator parameter, e and m are the electron charge and mass, respectively, and c is the speed of light. Hereinafter, we assume that $\gamma \gg 1$ and $K/\gamma \ll 1$. Consider a plane monochromatic wave $E_x = E\cos(kz - \omega t)$, with $k = \omega/c$, propagating in the direction of the z-axis (Fig. 7). We will treat this wave as a weak perturbation which barely changes the electron trajectory. To find the applicability criterion for this approximation, it is convenient to move to the attached frame of reference moving along the z-axis with the average electron velocity

$$\bar{v}_z \approx c\left(1 - \frac{1 + K^2/2}{2\gamma^2}\right) = c\left(1 - \frac{1}{2\gamma_\parallel^2}\right).$$

In the attached frame of reference, an electron oscillates in the field of two counterpropagating waves:[7]

$$E_{cx} = \frac{E}{2\gamma_\parallel}\cos\left[\frac{k}{2\gamma_\parallel}(z - ct)\right] + \gamma_\parallel B\cos\left[\gamma_\parallel k_w\left(z + \bar{v}_z t\right)\right]. \tag{5}$$

Therefore, the weakness criterion for an electromagnetic wave has the form $E \ll 2\gamma_\parallel^2 B$, which is fulfilled in most practically interesting cases.

The work done by the wave field over the electron during its small displacement along the trajectory is $-eE_x\,\mathrm{d}x$. Then, the change in the electron energy $\varepsilon = \gamma mc^2$ can be written out in the form

$$\frac{\mathrm{d}\varepsilon}{\mathrm{d}z} = -eE_x\frac{\mathrm{d}x}{\mathrm{d}z} \approx \frac{eEK}{\gamma}\cos(kz - \omega t)\sin(k_w z). \tag{6}$$

[6] Longitudinal plasma waves can have the phase velocity smaller than the electron velocity. It is such waves that are emitted by an electron moving uniformly and linearly.

[7] The motion of an electron in the field of counterpropagating waves and its relation to stimulated Compton scattering were investigated by P L Kapitza and P A M Dirac [5].

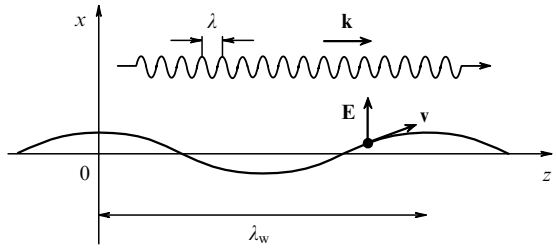

Figure 7. Electron moves along a cosine curve trajectory. A plane electromagnetic wave propagates along the z-axis.

Expression (6) was derived assuming that the wave field weakly affects the electron trajectory. We can choose the time of an electron arrival at a point with coordinate z as the second variable describing the electron motion. Then, one obtains

$$\frac{\mathrm{d}t}{\mathrm{d}z} = \frac{1}{v_z} = \frac{1}{\beta c}\sqrt{1 + \left(\frac{\mathrm{d}x}{\mathrm{d}z}\right)^2} \approx \frac{1}{c}\left[1 + \frac{1 + K^2/2}{2\gamma^2} - \frac{K^2}{4\gamma^2}\cos(2k_w z)\right]. \tag{7}$$

The system of differential equations (6) and (7) completely describes the longitudinal motion of an electron in the undulator under the action of an electromagnetic wave. These equations look rather complex, but their physical sense will be clear after their simplification, and the character of solution will become obvious. The right-hand side of equation (6), which can be called the effective longitudinal force, is proportional to

$$\cos(kz - \omega t)\sin(k_w z) = \frac{1}{2}\sin\left[(k + k_w)z - \omega t\right] - \frac{1}{2}\sin\left[(k - k_w)z - \omega t\right], \tag{8}$$

i.e., is the sum of two traveling waves. The first term on the right-hand side of formula (8) has the phase velocity $\omega/(k + k_w) = c/(1 + k_w/k)$, which is smaller than the speed of light, while the phase velocity of the second term is $\omega/(k - k_w) = c/(1 - k_w/k)$, i.e., is greater than the speed of light.[8] If an electron moves along the z-axis with the slow wave velocity, the contribution of the first term on the right-hand side of expression (8) to the longitudinal force (6) will be constant and can significantly change the electron energy at a long enough undulator length. We will call the energy of such an electron synchronous and write out the velocity-equality condition, called the phase-matching condition, by replacing the electron velocity with its value averaged over the undulator period (7):

$$c\left(1 - \frac{1 + K^2/2}{2\gamma^2}\right) = c\,\frac{k}{k + k_w}, \tag{9}$$

or

$$\lambda \approx \lambda_w\,\frac{1 + K^2/2}{2\gamma^2}. \tag{10}$$

[8] We can say that periodic modulation of the electron interaction with a wave [see formula (6)] produces the fast and slow spatial harmonics in the effective longitudinal force, as in the periodic accelerating structures of linear accelerators of charged particles and periodic decelerating systems of traveling wave tubes [3, 6].

A simple explanation of the phase-matching condition is as follows. Because the electric field is directed along the x-axis, the electron energy changes in the inclined sections of the trajectory. Assume that the electron flies through some place, for example, $z = \lambda_w/4$ at the instant when the wave field in this place is maximal, for example, at $t = \lambda_w/(4c)$. Then, the power transferred to the electron is $eEvK/\gamma$. The electron will get to a point $\lambda_w/2$ apart after a lapse of time $\lambda_w/(2\bar{v}_z)$. Simultaneously, the phase of a force acting on the electron from the wave side will change by

$$k\,\frac{\lambda_w}{2} - \omega\,\frac{\lambda_w}{2\bar{v}_z} = k\,\frac{\lambda_w}{2}\left(1 - \frac{c}{\bar{v}_z}\right) = \pi\,, \tag{11}$$

i.e., when phase-matching condition (10) is fulfilled, the force changes its sign. But the transverse component of the velocity also has another sign at this point. As a result, the transferred power remain the same. Thus, the electron will be accelerated along the entire undulator (until the break of the phase-matching condition caused by the energy increase). On the contrary, another electron with the same (synchronous) energy, but lagging behind the first one in time by π/ω, will be decelerated all the time.

Formula (10) coincides with the expression for the wavelength of spontaneous undulator radiation (see, for example, Ref. [1]) emitted at the zero angle (forward radiation). This coincidence, is, of course, not accidental. If we represent a free (without charges) electromagnetic field as a sum of many plane waves with different wave vectors and polarizations, then radiation appears from the action of a charge on these plane waves (field oscillators), the energy being transferred from a charged particle to each wave. Expression (6) describes the action of the wave on a charge. In both cases, the phase-matching condition provides a considerable energy transfer for a relatively long time. If the phase-matching condition is not fulfilled, the rate of energy transfer from a particle to the wave (and back) changes its sign all the time and the total energy transfer is small. Notice that the model of the radiation field as a set of independent plane waves greatly differs from the concept of the radiation field as a 'broken away' part of an electrostatic field. In classical electrodynamics, these two models agree with each other, and their alternating application allows one to understand better the physics of various phenomena. Quantum electrodynamics is based on the model of independent waves and this probably leads to some contradictions.

Returning to the phase-matching condition, we assume that it is fulfilled approximately for the energy ε, i.e., $\varepsilon = \varepsilon_s(1 + \delta)$, where

$$\frac{\varepsilon_s}{mc^2} = \gamma_s = \sqrt{\frac{(1 + K^2/2)\lambda_w}{2\lambda}}, \qquad \delta \ll 1\,.$$

We express the arrival time t in terms of the slow (because of the approximate fulfillment of the phase-matching condition) phase of the synchronous wave (the phase of the slow spatial harmonic):

$$\varphi = (k + k_w)z - \omega t - kK^2\,\frac{\sin(2k_w z)}{8k_w\gamma_s^2} + \pi\,.$$

We can say that $\varphi - \pi$ is the phase of the effective longitudinal force averaged over the undulator period and acting on an electron. Finally, we will measure the undulator length in periods divided by 2π, i.e., introduce the dimensionless independent variable $\zeta = k_w z$. After these replacements and omission of rapidly oscillating (with the undulator period) terms on the right-hand side of expression (6), equations (6) and (7) of the longitudinal motion of electrons will take a simple form

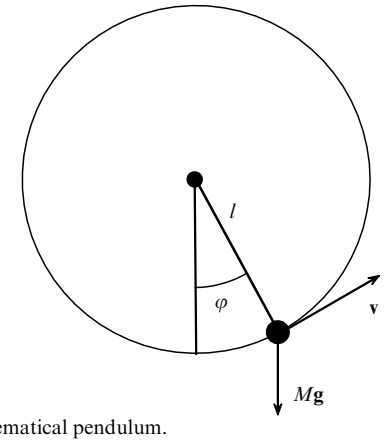

Figure 8. Mathematical pendulum.

$$\frac{d\delta}{d\zeta} = -A\sin\varphi\,, \tag{12}$$

where

$$A = \frac{eE\lambda K}{2\pi mc^2(1 + K^2/2)}\left[J_0\left(\frac{K^2}{4 + 2K^2}\right) - J_1\left(\frac{K^2}{4 + 2K^2}\right)\right]$$

(J_0 and J_1 are Bessel functions), and

$$\frac{d\varphi}{d\zeta} = 2\delta\,. \tag{13}$$

The system of differential equations (12) and (13) can be written out in the form of one second-order differential equation

$$\frac{d^2\varphi}{d\zeta^2} + 2A\sin\varphi = 0\,. \tag{14}$$

The behavior of solutions of these equations can be easily analyzed by the standard methods of mechanics, but we will also apply the mechanical analogy — the so-called mathematical pendulum — a small weight of mass M rotating around a hinge on a rod of length l (Fig. 8).

The equations of motion of such a pendulum, $dv/dt = -g\sin\varphi$ (Newton's second law) and $d\varphi/dt = v/l$, coincide accurate to within the notation with longitudinal motion equations (12) and (13). The total energy $M[v^2/2 + gl(1 - \cos\varphi)]$ of the mathematical pendulum is preserved. Therefore, if we draw constant-energy lines in the plane of dynamic variables — the velocity v and angle φ (Fig. 9) — then the pendulum motion will be depicted by the motion of a point in this phase plane along one of the constant-energy lines.

The phase trajectory of the oval shape corresponds to the oscillatory motion. The wavy lines correspond to rotation: the upper ones — counterclockwise (because $v > 0$), and the lower ones — clockwise. Two cosine curves separate closed phase trajectories (oscillations) from unclosed trajectories (rotations), i.e., form a separatrix. They depict the motion of the pendulum with the total energy $2Mgl$, stopping at the top position (i.e., at $\varphi = \pm\pi$). Notice that these equations (12)–(14) describe the longitudinal motion in linear accelerators of charged particles [6].

Despite the qualitatively simple behavior of the solutions of system (12), (13), its exact solutions is expressed in terms of

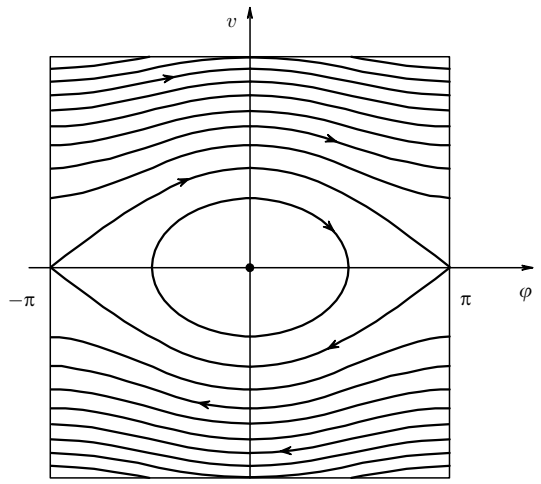

Figure 9. Phase trajectories of a mathematical pendulum. The arrows indicate the direction of motion along phase trajectories.

Jacobi elliptic functions (see, for example, book [7]). A simple analytical solution can be obtained for a small electromagnetic wave amplitude A. The solution can then be represented as a series over the parameter A:

$$\delta(\zeta) = \delta^{(0)}(\zeta) + A\delta^{(1)}(\zeta) + A^2\delta^{(2)}(\zeta) + \ldots,$$
$$\varphi(\zeta) = \varphi^{(0)}(\zeta) + A\varphi^{(1)}(\zeta) + A^2\varphi^{(2)}(\zeta) + \ldots. \quad (15)$$

The superscripts in parentheses show that these are different functions (these functions could be denoted by different letters). By substituting this expansion into the system being solved and equating the factors at the same powers of A on the left-hand and right-hand sides, we can find successively the zeroth-, first-, and higher-order solutions.

Let us now refine the physical formulation of the problem. It is very similar to that we discussed for an ensemble of emitting oscillators. Assume that electrons with the uniform phase distribution are flying into an undulator. For example, they can fly in with equal time intervals not multiple of the wave period $2\pi/\omega$. We assume that the energy of these electrons is the same: $\varepsilon_0 = \varepsilon_s(1 + \delta_0)$. The mean change in the electron energy at the output of the undulator of length $L = q\lambda_w$, i.e., at $\zeta = k_w L = 2\pi q$, should be found. To do this, the solution of system (12), (13) with the initial conditions δ_0, φ_0 must be found and then δ must be averaged over φ_0.

The subsequent calculations could be omitted, but we will see that they help to elucidate the process of producing the stimulated undulator radiation. After substituting expansions (15) into equations (12) and (13), they take the form

$$\frac{d\delta^{(0)}}{d\zeta} + A\frac{d\delta^{(1)}}{d\zeta} + A^2\frac{d\delta^{(2)}}{d\zeta} + \ldots$$
$$= -A\sin(\varphi^{(0)} + A\varphi^{(1)} + A^2\varphi^{(2)} + \ldots)$$
$$= -A\sin\varphi^{(0)} - A^2\varphi^{(1)}\cos\varphi^{(0)} + \ldots, \quad (16)$$
$$\frac{d\varphi^{(0)}}{d\zeta} + A\frac{d\varphi^{(1)}}{d\zeta} + A^2\frac{d\varphi^{(2)}}{d\zeta} + \ldots$$
$$= 2\delta^{(0)}(\zeta) + 2A\delta^{(1)}(\zeta) + 2A^2\delta^{(2)}(\zeta) + \ldots \quad (17)$$

In the zeroth order over the dimensionless wave amplitude A, i.e., at $A = 0$, energy is constant , i.e., $\delta^{(0)}(\zeta) = \delta_0$. Then, the integration of equation (17) gives $\varphi^{(0)}(\zeta) = \varphi_0 + 2\delta_0\zeta$.

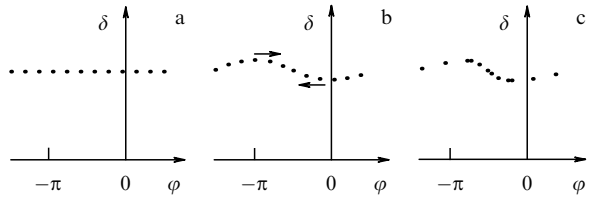

Figure 10. Change in the energy of particles moving in an undulator under the action of an accompanying electromagnetic wave. (a) The initial state. All the electrons have the same energies and are uniformly distributed over phase (i.e., over the time of entering the undulator). (b) Some particles lose their energy, while others acquire it. The phase distribution is still almost uniform, but due to the energy dependence of the frequency, phases begin to shift, as shown by arrows. (c) The phase shift gives rise to a crowding near the phase $-\pi/2$, and a rarefaction near the phase $\pi/2$.

This equality shows that particles with the greater energy move faster than a synchronous particle; therefore, the phase φ of the force acting on them increases. By substituting $\varphi^{(0)}$ into Eqn (16), we find

$$\delta^{(1)} = -\int_0^\zeta \sin\left[\varphi^{(0)}(\zeta')\right] d\zeta' = -\frac{\sin(\delta_0\zeta)\sin(\varphi_0 + \delta_0\zeta)}{\delta_0}. \quad (18)$$

The electron dynamics is clearly presented in Fig. 10, similar to Fig. 6.

It can be seen from formula (18) that in the first order one half of the particles ($0 \leqslant \varphi_0 + \delta_0\zeta < \pi$) lose their energy, while the other half acquires it (Fig. 10b), and on average the energy exchange between electrons and the wave is absent. This is quite understandable — our first approximation does not take into account the grouping of particles yet, which appears (Fig. 10c) in the same first approximation because of the first-order correction to the energy of particles:

$$\varphi^{(1)} = 2\int_0^\zeta \delta^{(1)}(\zeta')\, d\zeta' = \frac{\sin(\varphi_0 + 2\delta_0\zeta) - \sin\varphi_0}{2\delta_0^2} - \frac{\zeta\cos\varphi_0}{\delta_0}. \quad (19)$$

The dependence of grouping on the initial phase can be found from the expression

$$\frac{d\varphi}{d\varphi_0} \approx \frac{d\varphi^{(0)}}{d\varphi_0} + A\frac{d\varphi^{(1)}}{d\varphi_0}$$
$$= 1 + A\left[\frac{\cos(\varphi_0 + 2\delta_0\zeta) - \cos\varphi_0}{2\delta_0^2} + \frac{\zeta\sin\varphi_0}{\delta_0}\right]. \quad (20)$$

This quantity shows how many times the initial-phase interval $d\varphi_0$ is stretched. Because the number of particles within this interval is preserved, the initial density of particles (proportional to the instant electron-beam current) decreases by the same number of times. Taking the grouping into account, the number of decelerated and accelerated particles will be different, and the mean energy will change along the undulator. This is seen from the second-order correction

$$\delta^{(2)} = -\int_0^\zeta \varphi^{(1)}(\zeta')\cos\left[\varphi^{(0)}(\zeta')\right] d\zeta'$$
$$= \frac{1}{4\delta_0^3}\left[\cos(2\delta_0\zeta) - 1 + 2\delta_0\zeta\cos^2\varphi_0\sin(2\delta_0\zeta)\right.$$
$$\left. + 2\delta_0\zeta\sin\varphi_0\cos\varphi_0\cos(2\delta_0\zeta)\right] - \frac{\sin(2\delta_0\zeta)\sin(2\varphi_0 + 2\delta_0\zeta)}{8\delta_0^3}, \quad (21)$$

from which follows the energy change averaged over the initial phases:

$$\langle\delta-\delta_0\rangle=\frac{1}{2\pi}\int_0^{2\pi}\bigl(\delta(\varphi_0,\delta_0)-\delta_0\bigr)\,\mathrm{d}\varphi_0\approx A^2\langle\delta^{(2)}\rangle$$
$$=A^2\zeta^3\,\frac{\cos(2\delta_0\zeta)-1+\delta_0\zeta\sin(2\delta_0\zeta)}{4(\delta_0\zeta)^3}\,. \qquad (22)$$

Using expression (18), we can calculate the root-mean-square deviation of energy from its initial value:

$$\bigl\langle(\delta-\delta_0)^2\bigr\rangle\approx A^2\bigl\langle(\delta^{(1)})^2\bigr\rangle=\frac{A^2}{2}\left(\frac{\sin(\delta_0\zeta)}{\delta_0}\right)^2. \qquad (23)$$

Expressions (22) and (23) give a simple relationship

$$\langle\delta-\delta_0\rangle=\frac{1}{2}\,\frac{\mathrm{d}\bigl\langle(\delta-\delta_0)^2\bigr\rangle}{\mathrm{d}\delta_0}\,, \qquad (24)$$

which is called the Madey theorem [8, 9]. Equality (24) has an interesting physical meaning, which we will discuss briefly in Section 4.

4. Classical analog of Einstein relations

The system of equations of motion (12), (13) can be represented by Hamiltonian equations

$$\frac{\mathrm{d}\delta}{\mathrm{d}\zeta}=-\frac{\partial H(\delta,\varphi)}{\partial\varphi}\,,$$
$$\frac{\mathrm{d}\varphi}{\mathrm{d}\zeta}=\frac{\partial H(\delta,\varphi)}{\partial\delta}\,. \qquad (25)$$

For the system of equations (12) and (13), we have $H=\delta^2-A\cos\varphi$, with $\delta=I$ being the action for the 'unperturbed' (at $A=0$) system. Relationship (24) is fulfilled for a broad class of Hamiltonian systems described in action–angle variables [10, 11]. Its geometrical sense is that the area $\int_0^{2\pi}I(\varphi)\,\mathrm{d}\varphi=2\pi I_0$ under the curve in the phase space, on which the points depicting individual particles lie (see Fig. 10) remains constant (Liouville's theorem). Indeed, the condition of the conservation of the phase density during a small change in momenta and coordinates can be written out in terms of the transformation Jacobian:

$$1=\begin{vmatrix}\dfrac{\partial I}{\partial I_0} & \dfrac{\partial I}{\partial\varphi_0}\\[2mm] \dfrac{\partial\varphi}{\partial I_0} & \dfrac{\partial\varphi}{\partial\varphi_0}\end{vmatrix}\approx 1+\frac{\partial(I-I_0)}{\partial I_0}+\frac{\partial(\varphi-\varphi_0)}{\partial\varphi_0}\,. \qquad (26)$$

Then, one obtains

$$\langle I-I_0\rangle=\frac{1}{2\pi}\int_0^{2\pi}(I-I_0)\,\mathrm{d}\varphi_0=\frac{1}{2\pi}\int_0^{2\pi}I\left(1-\frac{\partial\varphi}{\partial\varphi_0}\right)\mathrm{d}\varphi_0$$
$$\approx\frac{1}{2\pi}\int_0^{2\pi}(I-I_0)\,\frac{\partial(I-I_0)}{\partial I_0}\,\mathrm{d}\varphi_0=\frac{1}{2}\,\frac{\mathrm{d}\bigl\langle(I-I_0)^2\bigr\rangle}{\mathrm{d}I_0}\,, \qquad (27)$$

which generalizes relation (24) for the case of an arbitrary one-dimensional autonomous Hamiltonian system. Using the dependence of the emitter energy $W(I)$ on the action I ($\Omega=\mathrm{d}W/\mathrm{d}I$ is the eigenfrequency), we arrive at

$$\langle\Delta W\rangle=\Omega\langle\Delta I\rangle=\Omega\,\frac{1}{2}\,\frac{\mathrm{d}\bigl\langle(\Delta I)^2\bigr\rangle}{\mathrm{d}I}=\frac{1}{2}\,\Omega^2\,\frac{\mathrm{d}\bigl(\Omega^{-2}\bigl\langle(\Delta W)^2\bigr\rangle\bigr)}{\mathrm{d}W}$$
$$=\frac{1}{2}\,\frac{\mathrm{d}\bigl\langle(\Delta W)^2\bigr\rangle}{\mathrm{d}W}-\bigl\langle(\Delta W)^2\bigr\rangle\,\frac{\mathrm{d}\ln\Omega}{\mathrm{d}W}\,. \qquad (28)$$

The change in the energy of an elementary emitter with the known current distribution $\mathbf{j}(\mathbf{r},t-t_1)$ under the action of a plane monochromatic wave $E_x=E\cos(kz-\omega t)$ can be expressed in the form

$$\Delta W=E\,\mathrm{Re}\int_{-\infty}^{\infty}\int j_x\exp\bigl[-\mathrm{i}(kz-\omega t-\omega t_1)\bigr]\,\mathrm{d}V\,\mathrm{d}t$$
$$=E\,\mathrm{Re}\bigl[\exp(\mathrm{i}\omega t_1)(j_x)_{\omega,k}\bigr]\,. \qquad (29)$$

Averaging over the emitter 'switching on' moments gives

$$\bigl\langle(\Delta W)^2\bigr\rangle=\frac{E^2}{2}\,\bigl|(j_x)_{\omega,k}\bigr|^2. \qquad (30)$$

Because, in the absence of an external wave, the spectral energy density emitted parallel to the z-axis and polarized along the x-axis (in the electric field direction) has the form

$$\frac{\mathrm{d}W_{\mathbf{n},\omega}}{\mathrm{d}o\,\mathrm{d}\omega/(2\pi)}=\frac{k^2}{2\pi c}\,\bigl|(j_x)_{\omega,k}\bigr|^2, \qquad (31)$$

where $\mathrm{d}o$ is the solid angle element, the mean square of the change in the emitter energy under the action of the external wave can be expressed in terms of the spectral density of spontaneous emission energy:

$$\bigl\langle(\Delta W)^2\bigr\rangle=\frac{\pi cE^2}{k^2}\,\frac{\mathrm{d}W_{\mathbf{n},\omega}}{\mathrm{d}o\,\mathrm{d}\omega/(2\pi)}\,. \qquad (32)$$

By substituting Eqn (32) into (28), we obtain

$$\langle\Delta W\rangle=\frac{\pi cE^2}{2k^2}\,\frac{\mathrm{d}}{\mathrm{d}W}\,\frac{\mathrm{d}W_{\mathbf{n},\omega}}{\mathrm{d}o\,\mathrm{d}\omega/(2\pi)}-\frac{\pi cE^2}{k^2}\,\frac{\mathrm{d}W_{\mathbf{n},\omega}}{\mathrm{d}o\,\mathrm{d}\omega/(2\pi)}\,\frac{\mathrm{d}\ln\Omega}{\mathrm{d}W}\,. \qquad (33)$$

Let us assume that the emitter operates at the average frequency ν. Then, the spectral intensity of spontaneous emission is given by

$$\frac{\mathrm{d}I_{\mathbf{n},\omega}}{\mathrm{d}o\,\mathrm{d}\omega/(2\pi)}=\nu\,\frac{\mathrm{d}W_{\mathbf{n},\omega}}{\mathrm{d}o\,\mathrm{d}\omega/(2\pi)}\,, \qquad (34)$$

and the radiation absorption cross section is

$$\sigma=\frac{8\pi\nu\langle\Delta W\rangle}{cE^2}=\lambda^2\,\frac{\mathrm{d}}{\mathrm{d}W}\,\frac{\mathrm{d}I_{\mathbf{n},\omega}}{\mathrm{d}o\,\mathrm{d}\omega/(2\pi)}-2\lambda^2\,\frac{\mathrm{d}I_{\mathbf{n},\omega}}{\mathrm{d}o\,\mathrm{d}\omega/(2\pi)}\,\frac{\mathrm{d}\ln\Omega}{\mathrm{d}W}\,. \qquad (35)$$

Formula (35) relating spontaneous emission to stimulated processes — absorption and amplification (for $\sigma<0$) — is the classical analog of relations between Einstein coefficients describing the probabilities of spontaneous and stimulated transitions. For narrowband emitters, in particular, for FELs considered in Refs [8, 9], the second term on the right-hand side of formula (35) can be disregarded.

5. Small-signal gain

Returning to explicit expression (22) for the energy change, we see that this quantity highly depends on the initial energy deviation δ_0 from the synchronous energy (Fig. 11). For positive deviations, particles lose their energy on average, whereas for negative deviations they acquire it. In other

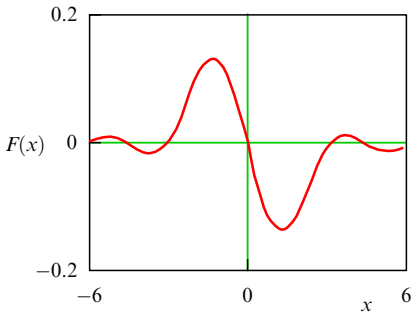

Figure 11. Function $F(x) = [\cos(2x) - 1 + x\sin(2x)]/(4x^3)$ of $x = \delta_0\zeta$, describing the dependence of the average change in electron energy on the electron initial energy.

words, the 'whirl' of a phase liquid shown in Fig. 9 slightly 'pulls in' particles located above and below the separatrix.[9] To provide the maximum energy extraction from particles, it is necessary to choose the initial energy deviation $\delta_0 = 1.3/\zeta$ corresponding to the minimum of function (22). In this case, $F(\delta_0\zeta) \approx -0.135$ and

$$\langle\delta - \delta_0\rangle_{\min} = -0.135A^2\zeta^3\,. \tag{36}$$

Such a dependence on the wave amplitude and the undulator length is almost obvious. Indeed, first the modulation of the particle energy takes place, which is proportional to the wave amplitude and the undulator length (we can suppose that this occurs in the first half of the undulator). Then, particles with the higher energy catch up with the lower energy particles, the resulting modulation of the longitudinal density being proportional to the energy modulation and length, i.e., to $A\zeta^2$. In the second half of the undulator, crowdings are decelerated, while rarefactions are accelerated proportionally to $A\zeta$, as during the energy modulation in the first half. The mean decrease in the electron energy is proportional to the density modulation and the energy modulation in the second half of the undulator.

Expression (36) also gives the electron efficiency $\eta = -\langle\delta - \delta_0\rangle_{\min}$ of a device, i.e., the fraction of the electron beam power $\varepsilon I/e$ transformed into radiation. To estimate the maximum efficiency, we will estimate the maximum dimensionless wave amplitude A. To do this, note that the previous consideration was obtained by the successive approximation method with expansion (15), which is valid when $|A\varphi^{(1)}| < \pi$. By using formula (19), we obtain $A\zeta^2 < \pi$ and $\eta_{\max} \sim 1/\zeta \approx 1/(2\pi q)$. Because usually $q \gg 1$, the FEL efficiency is low.

If the current of an electron beam flying through an undulator is I, i.e., I/e electrons pass through the undulator per second, then the beam gives away the power

$$P = -\frac{I}{e}\,\gamma mc^2\langle\delta - \delta_0\rangle = -F(2\pi q\delta_0)(4\pi)^2\lambda^2\left(\frac{K}{1+K^2/2}\right)^2 \times \left[J_0\left(\frac{K^2}{4+2K^2}\right) - J_1\left(\frac{K^2}{4+2K^2}\right)\right]^2 \frac{I}{I_A}\,\gamma q^3 c\,\frac{E^2}{8\pi} \tag{37}$$

to the wave, which is proportional to the intensity $cE^2/(8\pi)$ of the external wave. The constant $I_A = mc^3/e \approx 17$ kA is called the Alfvén current. If the wave appears to us as a light beam with the cross section S, its power is described by the expression $P_{\text{in}} = cE^2S/(8\pi)$. We assume that the electron beam is inside the light beam near the axis of the latter. The amplification of the light wave power in the undulator can then be described by the so-called small-signal gain:

$$G = \frac{P_{\text{out}} - P_{\text{in}}}{P_{\text{in}}} = \frac{8\pi P}{cE^2S} \approx -F(2\pi q\delta_0)(4\pi)^2\left(\frac{K}{1+K^2/2}\right)^2 \times \left[J_0\left(\frac{K^2}{4+2K^2}\right) - J_1\left(\frac{K^2}{4+2K^2}\right)\right]^2 \frac{\lambda^2}{S}\,\frac{I}{I_A}\,\gamma q^3\,. \tag{38}$$

It should be noted that this expression is valid only for the weak gain $G \ll 1$, because we derived it assuming that the wave amplitude A is invariable. Small-signal gain (38) is related to absorption cross section (35) by the relation $G = -\sigma/S$. Formula (38) also describes the amplification of a plane electromagnetic wave in a very broad electron beam with the current density $j = I/S$.

Small-signal gain (38) depends on the relative deviation of the electron energy from the energy ε_s at which phase-matching condition (10) is exactly fulfilled. On the other hand, we can assume that the electromagnetic-wave frequency ω deviates from the ω_0 value following from condition (10) for the energy $\varepsilon_0 = \varepsilon_s(1 + \delta_0)$ by the value of $(\omega - \omega_0)/\omega_0 = -2\delta_0$. Then, the first factor in formula (38) takes the form $-F[\pi q(\omega_0 - \omega)/\omega_0]$ and we obtain the frequency dependence of the gain with the maximum at the frequency $\omega_m = \omega_0(1 - 2.6/\zeta)$ and the relative width of about $1/q$.

The amplifier of electromagnetic radiation described above is called *a free electron laser*. Such a name can be explained by the fact that lasers of other types use the radiation of bound electrons, i.e., electrons bound in their atoms or crystals (in semiconductor lasers). Of course, electrons in FELs are also not completely free. To interact efficiently with an electromagnetic wave (to emit), they move in a magnetic field along a nonrectilinear trajectory (therefore, with acceleration). The common feature of all lasers is the exploitation of stimulated emission, i.e., the 'correct' phase-matching of individual emitters by the amplified wave. This phase-matching in FELs occurs due to the longitudinal bunching of electrons.

The 'relatives' of FELs in the longer-wavelength (centimeter) range are traveling wave tubes (TWTs) [3], where electrons are indeed 'free'. Moving along a straight line, electrons interact with a slow longitudinal electromagnetic wave, which can be formed, for example, in a hollow metal cylinder partially filled with a dielectric (Fig. 12).

The electric field of such a wave is longitudinal and changes the electron energy even without an undulator. The dielectric reduces the phase velocity of the wave to the electron velocity (i.e., the phase-matching condition is also

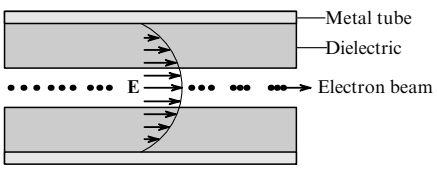

Figure 12. Schematic of a traveling wave tube with a waveguide filled with a dielectric.

[9] Because we assume that the dimensionless amplitude A of the electromagnetic wave is small, the separatrix height $\delta_{\max} = \sqrt{2A}$ is also small compared to δ_0.

fulfilled in TWTs). As in FELs, the longitudinal bunching occurs in TWTs. We can say that the TWT differs from the FEL only by the type of radiation used: undulator radiation in the FEL, and Cherenkov radiation in the TWT. The TWT gain is usually high, and the low-gain case is of no interest in practice. Nevertheless, expressions for the average energy change (22) are presented in old textbook [12] and are reproduced in Ref. [3].

6. Simplest FEL oscillator

To obtain the maximum gain, it is necessary to minimize the light-beam area S, as follows from formula (38). Obviously, by decreasing the area for a specified light wave power, we increase the radiation intensity and, therefore, the amplitude of the wave interacting with an electron. In this case, it is possible to extract the greater energy from the electron. At low frequencies, a metal waveguide can be used, for example, a rectangular waveguide with lateral sizes $a \times b$ possesses $S \approx \pi ab/2$ for the H_{01} wave. In this case, it is necessary to change phase-matching condition (9) by adding the term $c\pi^2/(2k^2a^2)$ to its right-hand side, which takes into account the increase in the phase velocity in the waveguide for $ka \gg 1$, and to estimate energy losses on waveguide walls. In the empty space, there is a limit for reducing the light-beam area over the undulator length, $L = q\lambda_w$, determined by light diffraction. To estimate it, we consider the approximate solution of the wave equation called a Gaussian beam [13, 14]:

$$E_x = E\,\mathrm{Re}\left\{\frac{\mathrm{i}z_0}{z-\mathrm{i}z_0}\exp\left[\mathrm{i}(kz-\omega t)+\mathrm{i}\,\frac{k}{2}\,\frac{x^2+y^2}{z-\mathrm{i}z_0}\right]\right\}, \quad (39)$$

which is applied for $kz_0 \gg 1$. The parameter z_0 is called the Rayleigh length. Solution (39) describes a monochromatic light beam concentrated near the z-axis with the Gaussian intensity distribution (the root-mean-square sizes are $\sigma_x = \sigma_y = [(z_0 + z^2/z_0)/(2k)]^{1/2}$) and the effective area

$$S = \frac{4\pi P}{c\overline{E_x^2(0,0,z)}} = 2\pi\sigma_x^2 = \frac{\lambda(z_0+z^2/z_0)}{2}\,.$$

Because it is necessary to minimize the beam cross section in the interval $-L/2 < z < L/2$, we can choose $z_0 = L/2$, then the effective area is $S \approx \lambda L/2$. Taking this into account, we obtain from formula (38) a simple result

$$G_{\max} \approx 25\,\frac{K^2}{1+K^2/2}\left[J_0\left(\frac{K^2}{4+2K^2}\right)-J_1\left(\frac{K^2}{4+2K^2}\right)\right]^2\frac{I}{I_A}\frac{q^2}{\gamma}\,, \quad (40)$$

which significantly depends only on the beam current I, the electron energy γ, and the number q of undulator periods (this complex factor depending on K is usually about unity).

If light passes many times through this FEL amplifier, the light power can increase by a few orders of magnitude after many transits. The simplest way to achieve this is to mount two mirrors in front and behind the FEL amplifier, with the radii of curvature equal to those of the wave front of Gaussian beam (39): $z + z_0^2/z$ and lateral sizes exceeding a few times the Gaussian beam width σ_x, as illustrated in Fig. 13.

Such a pair of mirrors is often called an optical resonator, because the decay time $-2L_m/[c\ln(\rho_1\rho_2)]$ (L_m is the distance between mirrors, ρ_1 and ρ_2 are the reflection coefficients of the mirrors) of the electromagnetic wave in the space between

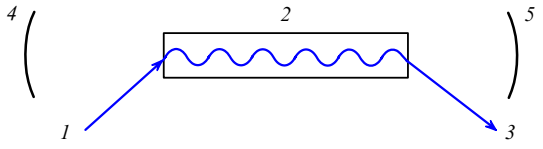

Figure 13. Schematic of an FEL oscillator. (*1*) input electron beam, (*2*) undulator, (*3*) waste electrons, (*4*, *5*) mirrors.

the mirrors greatly exceeds the wave period $2\pi/\omega$. This property resembles a high-Q oscillatory circuit or any other weakly decaying oscillator. The condition for increasing power has a simple form:

$$(1+G)\rho_1\rho_2 > 1\,, \quad (41)$$

i.e., the FEL gain should exceed mirror losses. If condition (41) is fulfilled, the power increases with time after 'switching on' an electron beam, the time of its increase by a factor of $e = 2.72$ being

$$\tau = \frac{2L_m}{c\ln[(1+G)\rho_1\rho_2]} \approx \frac{2L_m}{c(G+\rho_1+\rho_2-2)}$$

(the approximate equality is written out taking into account that $1-\rho \ll 1$, which follows from condition (41), and $G \ll 1$). Condition (41), called the lasing or self-excitation condition, is well known in radio engineering, describing an amplifier in which a part of the output signal (in our case $\rho_1\rho_2$) is fed to the amplifier input. This is called the positive-feedback amplification. For a strong enough feedback, when inequality (41) is wittingly fulfilled, the amplifier is 'self-excited', i.e., its noise (in our case, spontaneous radiation, as described below) is amplified by many orders of magnitude, even for the zeroth input signal. In other words, an amplifier with a strong enough positive feedback represents a self-excited oscillator. We can say that an FEL oscillator (see Fig. 13) consists of an FEL amplifier (see Fig. 1) and a pair of mirrors providing the positive feedback.

As mentioned above, a signal ceases to increase (due to so-called saturation) when the phase shifts of particles at the undulator end become close to unity. In this case, the beam at the undulator end is substantially periodically grouped, in the sense that the amplitude of the Fourier harmonic of the electron current with the electromagnetic-weave frequency ω becomes comparable to the average beam current I. This allows one to estimate the signal rise time from the instant of time the beam current is switched on until saturation, i.e., until the maximum power is reached. If the instants of time, at which electrons enter the undulator, are uncorrelated, the current is a pulsed stationary random process $I(t) = e\sum_i \delta(t-t_i)$ with the autocorrelation function $eI\delta(t_1-t_2)$ [15]. According to the Wiener–Khinchin theorem, its spectral power is the Fourier transform of the autocorrelation function, i.e., eI (at the nonzero frequency). After switching on the FEL, the spectral power near the gain maximum frequency $\omega_{\max}$ increases proportionally to

$$\exp\left(\frac{t}{\tau(\omega)}\right) = \exp\left(ct\,\frac{G(\omega)+\rho_1+\rho_2-2}{2L_m}\right)$$
$$\approx \exp\left(\frac{t}{\tau(\omega_m)}\right)\exp\left(\frac{ct}{4L_m}\,\frac{\mathrm{d}^2G}{\mathrm{d}\omega^2}\bigg|_{\omega_m}(\omega-\omega_m)^2\right). \quad (42)$$

As a result, the mean square of the alternate current component at the undulator output is given by

$$\begin{aligned}\overline{I^2(t)} &= 2eI\exp\left(\frac{t}{\tau(\omega_\mathrm{m})}\right)\\ &\times\int_0^\infty \exp\left(\frac{ct}{4L_\mathrm{m}}\left.\frac{\mathrm{d}^2G}{\mathrm{d}\omega^2}\right|_{\omega_\mathrm{m}}(\omega-\omega_\mathrm{m})^2\right)\frac{\mathrm{d}\omega}{2\pi}\\ &\approx \frac{2eI}{\sqrt{\pi}}\sqrt{\frac{L_\mathrm{m}}{ct}}\left(\left.\frac{\mathrm{d}^2G}{\mathrm{d}\omega^2}\right|_{\omega_\mathrm{m}}\right)^{-1/2}\exp\left(\frac{t}{\tau(\omega_\mathrm{m})}\right). \end{aligned} \tag{43}$$

Upon saturation, this quantity is on the order of I^2, and, therefore, the time during which saturation is reached can be estimated as

$$\begin{aligned}t_\mathrm{sat} &\approx \tau(\omega_\mathrm{m})\ln\left[\frac{I}{e}\sqrt{\frac{1}{G(\omega_\mathrm{m})+\rho_1+\rho_2-2}\left.\frac{\mathrm{d}^2G}{\mathrm{d}\omega^2}\right|_{\omega_\mathrm{m}}}\right]\\ &\approx \tau(\omega_\mathrm{m})\ln\left(\frac{I}{e}\frac{2\pi q}{\omega_\mathrm{m}}\right). \end{aligned} \tag{44}$$

The logarithm in formula (44) is usually approximately equal to 20, i.e., the saturation time is about 20 small-signal rise times by a factor of 2.72.

7. Restrictions on the electron beam parameters

We assumed in Sections 3–6 that all the electrons entering the FEL have the same initial velocities and coordinates but enter there at different instants of time. Real electron beams contain electrons with different velocities and coordinates. Let us estimate the limits of applicability of ignoring the coordinate and velocity dispersions. To do this, we consider the motion of an electron with deviations of initial conditions from some reference values. Because the action of the amplified wave is a small perturbation, we disregard it. As in formula (7), we will write the longitudinal velocity of the electron in the form

$$\begin{aligned}\overline{\beta_z} &= \frac{\overline{v_z}}{c} = \overline{\frac{\beta}{\sqrt{1+(\mathrm{d}x/\mathrm{d}z)^2+(\mathrm{d}y/\mathrm{d}z)^2}}}\\ &\approx 1-\frac{1+K^2(x,y)/2}{2\gamma^2}-\frac{1}{2}\left(\overline{\frac{\mathrm{d}x}{\mathrm{d}z}}\right)^2-\frac{1}{2}\left(\overline{\frac{\mathrm{d}y}{\mathrm{d}z}}\right)^2\\ &\approx 1-\frac{1+K^2(0,0)/2}{2\gamma_0^2}+\frac{1+K^2(0,0)/2}{\gamma_0^2}\frac{\gamma-\gamma_0}{\gamma_0}\\ &-\frac{1}{2}\left(\overline{\frac{\mathrm{d}x}{\mathrm{d}z}}\right)^2-\frac{1}{2}\left(\overline{\frac{\mathrm{d}y}{\mathrm{d}z}}\right)^2-\frac{1}{8\gamma_0^2}\frac{\partial^2K^2}{\partial x^2}\bar{x}^2-\frac{1}{8\gamma_0^2}\frac{\partial^2K^2}{\partial y^2}\bar{y}^2, \end{aligned} \tag{45}$$

where the over-bars mean averaging over the undulator period. The latter two terms take into account the transverse nonuniformity of the undulator field. For example, in a planar undulator with not too large a period, $K\propto\cosh(k_\mathrm{w}y)$ [1] and $\partial^2K^2/\partial y^2=2K^2(0,0)k_\mathrm{w}^2$, and $\partial^2K^2/\partial x^2=0$. Because the deviation $\Delta\beta_z$ of the longitudinal velocity leads to the departure of a particle ahead of the reference particle, the admissible dispersion of longitudinal velocities, according to qualitative considerations presented after expression (36), can be estimated from the inequality $|\Delta\beta_z|L/2<\lambda/(2\pi)$, or

$$|\Delta\beta_z|<\frac{\lambda}{\pi L}=\frac{1}{2\pi q\gamma_\parallel^2}. \tag{46}$$

Notice that [see formula (10)] inequality (46) specifies the condition that the relative shift in the spontaneous emission wavelength $|\Delta\lambda/\lambda|=\lambda_\mathrm{w}|\Delta\beta_z|/\lambda=2\gamma_\parallel^2|\Delta\beta_z|<1/(\pi q)$, i.e., is smaller than the relative width of the spontaneous undulator radiation spectrum. By substituting contributions of different terms from Eqn (45) into (46), we obtain restrictions on the root-mean-square energy and angle dispersions and on the rms sizes of the electron beam:

$$\frac{\sqrt{\langle(\gamma-\gamma_0)^2\rangle}}{\gamma_0}<\frac{1}{2\pi q}, \tag{47}$$

$$\sqrt{\left\langle\left(\overline{\frac{\mathrm{d}x}{\mathrm{d}z}}\right)^2\right\rangle},\sqrt{\left\langle\left(\overline{\frac{\mathrm{d}y}{\mathrm{d}z}}\right)^2\right\rangle}<\sqrt{\frac{1}{\sqrt{2}\pi q\gamma_\parallel^2}}=\sqrt{\frac{\sqrt{2}\lambda}{\pi L}}, \tag{48}$$

$$\begin{aligned}\sqrt{\langle\bar{x}^2\rangle} &< \sqrt{k_\mathrm{w}^2\frac{4+2K^2}{\partial^2K^2/\partial x^2}}\frac{\lambda_\mathrm{w}}{\pi\sqrt{2\pi q}},\\ \sqrt{\langle\bar{y}^2\rangle} &< \sqrt{k_\mathrm{w}^2\frac{4+2K^2}{\partial^2K^2/\partial y^2}}\frac{\lambda_\mathrm{w}}{\pi\sqrt{2\pi q}}. \end{aligned} \tag{49}$$

Inequality (48) requires that the angular dispersions of electrons should not exceed the diffraction divergence $\sqrt{\lambda/L}$ of spontaneous undulator radiation (see review [1]). Inequalities (49) should be supplemented by the condition that all the electrons be located inside the light beam, for example, the Gaussian mode of an optical resonator of size $\sqrt{\lambda L/(4\pi)}$:

$$\sqrt{\langle\bar{x}^2\rangle},\sqrt{\langle\bar{y}^2\rangle}<\sqrt{\frac{\lambda L}{4\pi}}. \tag{50}$$

By using a focusing device, for example, magnetic quadrupole lenses, we can reduce the lateral sizes of the electron beam to satisfy conditions (49) and (50). However, due to the conservation of transverse emittances (i.e., the projections of the phase volume occupied by electrons)

$$\varepsilon_x\approx\sqrt{\langle\bar{x}^2\rangle}\sqrt{\left\langle\left(\overline{\frac{\mathrm{d}x}{\mathrm{d}z}}\right)^2\right\rangle},\quad \varepsilon_y\approx\sqrt{\langle\bar{y}^2\rangle}\sqrt{\left\langle\left(\overline{\frac{\mathrm{d}y}{\mathrm{d}z}}\right)^2\right\rangle},$$

the angular dispersions will increase in this case. By multiplying inequalities (48) and (50), we see that the necessary condition for their fulfillment is the smallness of the emittances of the electron beam compared to the radiation wavelength:

$$\varepsilon_{x,y}<\frac{\lambda}{2\pi}. \tag{51}$$

8. High-gain free electron lasers

We considered above the FEL operation in the low-gain regime: $G\ll 1$. This condition is violated for a large enough length of the undulator. In particular, modern X-ray FELs use very long undulators (about 100 m long). As in any linear system, a monochromatic signal (radiation and the alternate component of the electron current) grows exponentially. In the simplest cases, the high-gain FEL regime is described by the same expressions as the high-gain TWT regime [3, 12, 20]. The length L_g at which the signal power increases by a factor of 2.72 (the so-called gain length) can be roughly estimated by equating gain (38) to unity. In such a rough model, a long FEL is replaced by a sequence of FELs of length L_g, for which the low-gain approximation is still applicable. Because the diffraction expansion of the X-ray beam is relatively small, we

replace the light beam area S by the electron beam area. Then, $I/S = j$ is the beam current density. As a result, we obtain

$$L_g \approx \frac{\lambda_w}{2} \sqrt[3]{\frac{2I_A}{(4\pi)^2 j\gamma\lambda^2}} \left(\frac{K}{1+K^2/2}\right)^{-2/3} = \frac{\gamma}{2} \sqrt[3]{\frac{I_A\lambda_w}{2\pi^2 jK^2}}. \quad (52)$$

Estimate (52) is valid for a small dispersion of the longitudinal electron velocities. Therefore, the fulfillment of conditions (47)–(49), (51), where $L = 2L_g$, is desirable for X-ray FELs. In particular, condition (51) restricts the electron energy from below, $\gamma > 2\pi\gamma\varepsilon_{x,y}/\lambda$, where $\gamma\varepsilon_{x,y}$ are normalized emittances, i.e., invariant (conserved during the acceleration of electrons) phase areas occupied by electrons (see, for example, Refs [6, 16]). In particular, at $\lambda = 0.1$ nm and $\gamma\varepsilon_{x,y} = 0.2$ μm, we have $E > 6$ GeV. The estimate of the electron efficiency mentioned after expression (36) gives $\eta \sim \lambda_w/(4\pi L_g)$ for high-gain FELs.

9. Work on free electron lasers at the Budker Institute of Nuclear Physics

The history of work on the development of FELs is quite completely described in book [3]. Here, we mention only some important events: the invention of an undulator by V L Ginzburg [17] in 1947, experiments of G Motz with undulator radiation [18, 19], and the creation of the first FEL — ubitron by R Phyllips in 1960 [20]. In 1976, the group of J Madey demonstrated the amplification of emission at a wavelength of 10.6 μm in an FEL with a helical superconducting undulator [21], and then the same group created an FEL oscillator emitting at 3.4 μm [22].

The FEL operation requires the use of a high-quality electron beam (i.e., with small lateral sizes and a small velocity dispersion) and high mean and peak currents. Moreover, the source of such a beam — an electron accelerator — is the most complex and expensive part of the FEL. Therefore, interest in FELs at the INP, SB USSR AS, where the development of charged particle accelerators was one of the main topics, was quite natural.

Theoretical FEL studies were performed at the Budker INP by several groups.

V N Baier and A I Milstein developed the FEL theory. They studied the low-gain [23] and high-gain [24, 25] regimes and the spectrum evolution after switching on amplification in an FEL with an optical resonator [26].

A M Kondratenko and E L Saldin obtained the equation for a high-gain FEL in free space taking diffraction effects into account [27–29] and investigated FELs with plane mirrors [30].

A N Skrinsky and N A Vinokurov proposed a higher-gain FEL modification — an optical klystron (OK) [31], studied the power restriction mechanism in an OK mounted on an electron storage ring [32], and proposed using a waveguide metal resonator with a small vertical aperture in a submillimeter FEL [33].

V N Litvinenko and N A Vinokurov calculated the radiation parameters of an FEL mounted on an electron storage ring [34], while V M Popik and N A Vinokurov calculated the radiation parameters of an FEL with a plane–parallel glass plate (a Fabry–Perot etalon) inside an optical resonator [35].

G N Kulipanov and colleagues pointed out the possibility of retaining the microbunching of an electron beam during an achromatic turning [36].

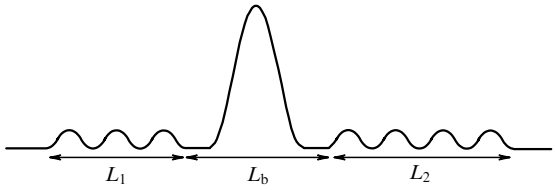

Figure 14. Electron trajectory in an optical klystron.

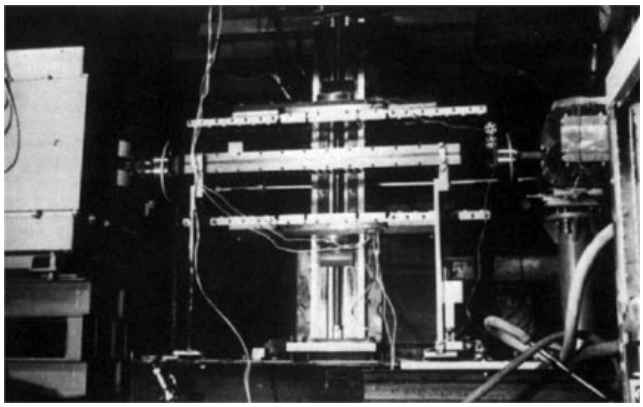

Figure 15. First magnetic system of an optical klystron operating on a VEPP-3 storage ring beginning in 1979. In the middle: a three-pole bunching wiggler with two undulators on the left and right, which were the world's first undulators with permanent magnets and a variable gap.

N A Vinokurov substantiated the possibility of using sectioned undulators in high-gain FELs [37], while O A Shevchenko and N A Vinokurov developed the correlation theory for high-gain FELs [38, 39] (similar to the Bogolyubov chain of equations) and compared its results with those of the quasilinear theory [40, 41].

Experimental work was initiated in 1979 when the first experiments with an OK were performed on a VEPP-3 electron–positron collider [42]. The device differs from a standard FEL by its undulator, divided into two parts of lengths L_1 and L_2 (Fig. 14) with a magnetic bunching device (a three-pole compensated wiggler with a large period L_b) to improve bunching.

The first OK, about 1 m in length, shown in Fig. 15, utilized the best permanent samarium–cobalt magnets manufactured at the Pyshminskii Giredmet pilot plant in Sverdlovsk region. The field was controlled by varying the working gap.

All the FELs with electron storage rings in the world were made by the OK scheme, providing much greater amplification compared to that in usual FELs.

Then, a series of experimental studies was performed resulting in the creation of the world's first UV FEL in 1988. During these studies, original technological solutions for undulators were proposed and realized, which are now used in all X-ray sources based on electron storage rings (a variable-gap undulator, a so-called hybrid undulator [43], etc. (see details in review [1]).

In 1988, a new OK-4 FEL mounted on a bypass (a specially made additional straight-line section) of the VEPP-3 storage ring was put into operation [44]. The use of a bypass made possible mounting a very long (7.5 m) FEL on the storage ring. The original design of this electromagnetic

undulator [45] proved to be successful and was later used in several undulators in Russia and abroad. Such a long undulator provided amplification sufficient for obtaining the record short UV wavelength of 0.24 μm and the record narrow spectrum (3×10^{-6}) [46] and also provided transverse mode locking in a confocal resonator [47]. The 'short-wavelength' persisted for more than 10 years. The same OK-4 setup was used for testing the coherence of spontaneous radiation from two undulators in tandem separated by an achromatic turn [48]. These experiments are important for producing the so-called electron outcoupling of radiation [49], solving the problem of radiation outcoupling from the optical resonator of a high-power FEL.

Along with FEL studies at the Budker INP, SB RAS, the Institute was involved in the development of the OK in the electron storage ring at Duke University (USA) [50, 51] and the development of a compact FEL at KAERI (Korea Atomic Energy Research Institute (South Korea) [52, 53].

10. High-power FEL at the Siberian Center of Photochemical Research

As mentioned in Section 5, the FEL electron efficiency is rather low (as a rule, no more than 1%). This is due to violation of the synchronism condition for decelerated electrons. The output power of FELs with storage rings is even more restricted due to the repeated interactions of electrons with the wave [32]. Because of this, A N Skrinsky and N A Vinokurov proposed creating high-power FELs using a special class of electron accelerators — high-frequency energy recovery linacs (ERLs). Electrons in ERLs are first accelerated in high-frequency resonators, then are used in the FEL (or for other aims), and decelerated in the same high-frequency resonators by returning the power spent for acceleration [55]. The employment of ERLs provides high average electron currents and considerably reduces the radiative danger of the setup.

The Laboratory of Laser Photochemistry headed by A K Petrov has long worked at the Institute of Chemical Kinetics and Combustion (ICKC), SB RAS. In the early 1990s, after a discussion of the potential of the high-power FEL at the INP and the ICKC (headed by Yu N Molin at that time), it was decided to create such a facility at the ICKC building No. 11, and to organize the Center of Photochemical Studies based on it. The first phase of this FEL was commissioned in 2003 [56].

At present, the unique Novosibirsk FEL facility includes three FELs (Fig. 16) emitting narrowband coherent radiation with a mean power of up to 500 W, a peak power exceeding 1 MW, and a wavelength continuously tunable in the range from 8 to 240 μm [57–61]. The mean power of 500 W is the world record for radiation sources in the terahertz frequency range. The parameters of three FELs are presented in the Table.

FEL radiation is outcoupled through a dry nitrogen-filled channel to a room for users, where it is distributed among experimental stations, where researchers from RAS, higher institutes of learning, and other institutions perform scientific studies in physics, biology, chemistry, and medicine. The use of high-power submillimeter tunable radiation opened fundamentally new possibilities for experimentalists. Thus, Russian scientists have received a unique tool for investigations — a facility of high-power FELs continuously tunable in the submillimeter and IR ranges.

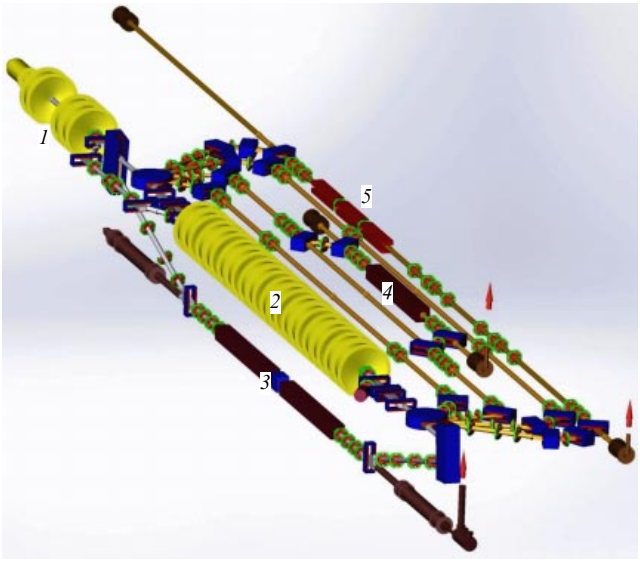

Figure 16. Schematic of the Novosibirsk FEL: (*1*) injector, (*2*) main accelerating resonators, (*3*) undulator of the first FEL, (*4*) undulator of the second FEL, and (*5*) undulator of the third FEL.

Table. Parameters of FELs commissioned in 2003, 2009, and 2015.

Parameters \ Range, start year	Terahertz range, 2003	Far IR, 2009	IR, 2015
Wavelength, μm	90 – 240	37 – 80	8 – 11
Spectrum width (FWHM), %	0.2 – 2.0	0.2 – 1	0.1 – 1
Maximum mean power, kW	0.5	0.5	0.1
Maximum peak power, MW	0.5	2.0	5
Pulse duration, ps	30 – 120	20 – 40	10 – 20
Pulse repetition rate, MHz	5.6	7.5	3.8

11. Conclusion

We have described the FEL operation principle. These electromagnetic radiation oscillators are simultaneously vacuum electronic devices and lasers. The use of ultrarelativistic electron beams with the gigawatt mean power density per mm^2 allows FELs emitting kilowatt mean powers in the wavelength range from 0.1 nm to 1 mm to be created. The discussion of the FEL operation principles and studies performed at the Budker INP, SB RAS in this field was brief because of the limited volume of the article. Some details can be found in reviews [62, 63]. The application of FELs for solving basic scientific and practical problems is beyond the scope of this paper.

Acknowledgments. This study was supported by the Russian Science Foundation (project No. 14-50-00080).

References

1. Vinokurov N A, Levichev E B *Phys. Usp.* **58** 850 (2015); *Usp. Fiz. Nauk* **185** 917 (2015)

2. Gorelik G S *Kolebaniya i Volny* (Oscillations and Waves) (Moscow: Fizmatlit, 1959)
3. Trubetskov D I, Khramov A E *Lektsii po Sverkhvysokochastotnoi Elektronike dlya Fizikov* (Lectures on Microwave Electronics for Physicists) (Moscow: Fizmatlit, 2004)
4. Landau L D *Zh. Eksp. Teor. Fiz.* **16** 574 (1946); Landau L D *J. Phys. USSR* **10** 25 (1946)
5. Kapitza P L, Dirac P A M *Proc. Cambr. Phil. Soc.* **29** 297 (1933)
6. Lebedev A N, Shal'nov A V *Osnovy Fiziki i Tekhniki Uskoritelei* (Fundamentals of the Physics and Technique of Accelerators (Moscow: Energoatomizdat, 1991)
7. Kauderer H *Nichtlineare Mechanik* (Berlin: Springer-Verlag, 1958); Translated into Russian: *Nelineinaya Mekhanika* (Moscow: IL, 1961)
8. Kolomenskii A A, Lebedev A N *Sov. J. Quantum Electron.* **8** 879 (1978); *Kvantovaya Elektron.* **5** 1543 (1978)
9. Madey J M J *Nuovo Cimento B* **50** 64 (1979)
10. Vinokurov N A Preprint No. 81-02 (Novosibirsk: Institute of Nuclear Physics of the Siberian Branch of the USSR Acad. of Sci., 1981); http://www.inp.nsk.su/activity/preprints/files/1981_002.pdf
11. Litvinenko V N, Vinokurov N A *Nucl. Instrum. Meth. Phys. Res. A* **331** 440 (1993)
12. Shevchik V N, Trubetskov D I *Analiticheskie Metody Rascheta v Elektronike SVCh* (Analytical Calculation Methods in Microwave Electronics) (Moscow: Sovetskoe Radio, 1970)
13. Yariv A *Quantum Electronics* (John Wiley and Sons, Inc., 1975); Translated into Russian: *Kvantovaya Elektronika* (Moscow: Sovetskoe Radio, 1980)
14. Vainshtein L A *Elektromagnitnye Volny* (Electromagnetic Waves) (Moscow: Radio i Svyaz', 1988)
15. Rytov S M, Kravtsov Yu A, Tatarskii V I *Principles of Statistical Radiophysics* Vols 1, 2 (Berlin: Springer-Verlag, 1987); Translated from Russian: *Vvedenie v Statisticheskuyu Radiofiziku* (Introduction to Statistical Radiophysics) Pt. 1 *Sluchainye Protsessy* (Random Processes) (Moscow: Nauka, 1976)
16. Vinokurov N A et al. *Phys. Usp.* **60** 1034 (2017); *Usp. Fiz. Nauk* **187** 1116 (2017)
17. Ginzburg V L *Izv. Akad. Nauk SSSR Ser. Fiz.* **11** 165 (1947)
18. Motz H *J. Appl. Phys.* **22** 527 (1951)
19. Motz H, Thon W, Whitehurst R N *J. Appl. Phys.* **24** 826 (1953)
20. Phyllips R N *IRE Tran. Electron Dev.* **7** 231 (1960)
21. Elias L R et al. *Phys. Rev. Lett.* **36** 717 (1976)
22. Deacon D A G et al. *Phys. Rev. Lett.* **38** 892 (1977)
23. Baier V N, Milstein A I *Phys. Lett. A* **65** 319 (1978)
24. Baier V N, Milstein A I *Sov. Phys. Dokl.* **25** 112 (1980); *Dokl. Akad. Nauk SSSR* **250** 1364 (1980)
25. Baier V N, Milstein A I *Phys. Lett. A* **79** 77 (1980)
26. Baier V, Milstein A *IEEE J. Quantum Electron.* **21** 1023 (1985)
27. Kondratenko A M, Saldin E L *Dokl. Akad. Nauk SSSR* **249** 843 (1979); Kondratenko A M, Saldin E L *Sov. Phys. Dokl.* **24** 986 (1979)
28. Kondratenko A M, Saldin E L *Particle Accelerators* **10** 207 (1980)
29. Kondratenko A M, Saldin E L *Zh. Tekh. Fiz.* **51** 1633 (1981)
30. Kondratenko A M, Saldin E L *Zh. Tekh. Fiz.* **52** 309 (1982)
31. Vinokurov N A, Skrinsky A N, Preprint No. 77-59 (Novosibirsk: Institute of Nuclear Physics of the Siberian Branch of the USSR Acad. of Sci., 1977); http://wwwold.inp.nsk.su/activity/preprints/files/1977_059.pdf
32. Vinokurov N A, Skrinsky A N, Preprint No. 77-67 (Novosibirsk: Institute of Nuclear Physics of the Siberian Branch of the USSR Acad. of Sci., 1977); http://wwwold.inp.nsk.su/activity/preprints/files/1977_067.pdf
33. Vinokurov N A, Skrinsky A N, in *Relyativistskaya Vysokochastotnaya Elektronika*: *Problemy Povysheniya Moshchnosti i Chastoty Izlucheniya* (Relativistic High-Frequency Electronics: Problems of Increasing Radiation Power and Frequency) (Gorky: Institute of Applied Physics of the USSR Acad. of Sci., 1981) p. 204
34. Litvinenko V N, Vinokurov N A *Nucl. Instrum. Meth. Phys. Res.A* **304** 66 (1991)
35. Popik V M, Vinokurov N A *Nucl. Instrum. Meth. Phys. Res. A* **341** abs134 (1994)
36. Kulipanov G N et al. *Nucl. Instrum. Meth. Phys. Res. A* **308** 106 (1991)
37. Vinokurov N A *Nucl. Instrum. Meth. Phys. Res. A* **375** 264 (1996)
38. Shevchenko O A, Vinokurov N A *Nucl. Instrum. Meth. Phys. Res. A* **507** 84 (2003)
39. Shevchenko O A, Vinokurov N A *Nucl. Instrum. Meth. Phys. Res. A* **603** 46 (2009)
40. Vinokurov N A et al. *Nucl. Instrum. Meth. Phys. Res. A* **475** 74 (2001)
41. Shevchenko O A, Vinokurov N A *Radiophys. Quantum Electron.* **60** 37 (2017); *Izv. Vyssh. Uchebn. Zaved. Radiofiz.* **60** 41 (2017)
42. Artamonov A S et al. *Nucl. Instrum. Meth. Phys. Res.* **177** 247 (1980)
43. Kornyukhin G A et al. *Nucl. Instrum. Meth. Phys. Res.* **208** 189 (1983)
44. Drobyazko I B A et al. *Nucl. Instrum. Meth. Phys. Res. A* **282** 424 (1989)
45. Gavrilov N G et al. *Nucl. Instrum. Meth. Phys. Res. A* **282** 422 (1989)
46. Couprie M E et al. *Nucl. Instrum. Meth. Phys. Res. A* **304** 47 (1991)
47. Kulipanov G N et al. *Nucl. Instrum. Meth. Phys. Res. A* **331** 98 (1993)
48. Gavrilov N G et al. *Nucl. Instrum. Meth. Phys. Res. A* **308** 109 (1991)
49. Gavrilov N G et al. *IEEE J. Quantum Electron.* **27** 2569 (1991)
50. Litvinenko V N et al. *Phys. Rev. Lett.* **78** 4569 (1997)
51. Litvinenko V N et al. *Nucl. Instrum. Meth. Phys. Res. A* **475** 247 (2001)
52. Akberdin R R et al. *Nucl. Instrum. Meth. Phys. Res. A* **405** 195 (1998)
53. Jeong Y U et al. *Nucl. Instrum. Meth. Phys. Res. A* **475** 47 (2001)
54. Vinokurov N A, Skrinskii A N, Preprint No. 78-88 (Novosibirsk: Institute of Nuclear Physics, SB USSR AS, 1978); http://wwwold.inp.nsk.su/activity/preprints/files/1978_088.pdf
55. Gavrilov N G et al. *Nucl. Instrum. Meth. Phys. Res. A* **304** 228 (1991)
56. Antokhin E A et al. *Nucl. Instrum. Meth. Phys. Res. A* **528** 15 (2004)
57. Kulipanov G N et al. *IEEE Trans. THz Sci. Technol.* **5** 798 (2015)
58. Shevchenko O A et al. *Phys. Part. Nucl. Lett.* **13** 1002 (2016)
59. Shevchenko O A et al. *Phys. Procedia* **84** 13 (2016)
60. Knyazev B A et al. *Phys. Procedia* **84** 27 (2016)
61. Shevchenko O A et al. *Radiophys. Quantum Electron.* **59** 605 (2017); *Izv. Vyssh. Uchebn. Zaved. Radiofiz.* **59** 671 (2016)
62. Vinokurov N A *Rev. Accel. Sci. Technol.* **3** 77 (2010)
63. Vinokurov N A *J. Infrared Millimeter Terahertz Waves* **32** 1123 (2011)